One of the proteins identified through this screen was CD44, a cell membrane-bound glycoprotein involved in cell adhesion and migration (*38*). The spatial organization of CD44 upon ephrin-A1 stimulation was found to antilocalize with the assembly of EphA2 (Fig. 4D), validating the involvement of CD44 in cell-driven EphA2 receptor reorganization. The system-wide correlation analysis does not necessarily provide the mechanistic details leading to EphA2 sorting; instead, it identifies proteins and genes that may serve as surrogate markers to centripetal transport.

In conclusion, we report a spatio-mechanical regulation of the EphA2 signaling pathway. Upon membrane-bound ligand stimulation, EphA2 is transported radially inwards by an actomyosin contractile process. Physical interference with this transport, which necessarily involves the imposition of opposing forces on EphA2, alters ligand-induced EphA2 activation as observed by the recruitment of the protease ADAM10 and cytoskeleton morphology. Quantitative measurement of centripetal receptor transport across a library of mammary epithelial cell lines reveals a high correlation with invasion potential and with specific gene and protein expression. These observations suggest that spatio-mechanical aspects of ephrin-A1 expressing cells and their surrounding tissue environment may functionally alter the response of EphA2 signaling systems and could play a contributing role in the onset and progression of cancer.

References and Notes

1. D. E. Discher, P. Janmey, Y.-l. Wang, *Science* **310**, 1139 (2005).
2. M. J. Dalby *et al.*, *Nat. Mater.* **6**, 997 (2007).
3. C. M. Nelson, M. M. VanDuijn, J. L. Inman, D. A. Fletcher, M. J. Bissell, *Science* **314**, 298 (2006).
4. D. T. Butcher, T. Alliston, V. M. Weaver, *Nat. Rev. Cancer* **9**, 108 (2009).
5. C. S. Chen, *J. Cell Sci.* **121**, 3285 (2008).
6. S. Y. Qi, J. T. Groves, A. K. Chakraborty, *Proc. Natl. Acad. Sci. U.S.A.* **98**, 6548 (2001).
7. K. D. Mossman, G. Campi, J. T. Groves, M. L. Dustin, *Science* **310**, 1191 (2005).
8. N. L. Andrews *et al.*, *Nat. Cell Biol.* **10**, 955 (2008).
9. S. Hurtley, *Science* **326**, 1205 (2009).
10. N. C. Hartman, J. A. Nye, J. T. Groves, *Proc. Natl. Acad. Sci. U.S.A.* **106**, 12729 (2009).
11. J. D. Scott, T. Pawson, *Science* **326**, 1220 (2009).
12. R. O. Hynes, *Science* **326**, 1216 (2009).
13. T. Marquardt *et al.*, *Cell* **121**, 127 (2005).
14. M. Lackmann, A. W. Boyd, *Sci. Signal.* **1**, re2 (2008).
15. K. Kullander, R. Klein, *Nat. Rev. Mol. Cell Biol.* **3**, 475 (2002).
16. J. Walker-Daniels, D. J. Riese II, M. S. Kinch, *Mol. Cancer Res.* **1**, 79 (2002).
17. P. W. Janes *et al.*, *Cell* **123**, 291 (2005).
18. S. Davis *et al.*, *Science* **266**, 816 (1994).
19. J. T. Groves, *Curr. Opin. Chem. Biol.* **10**, 544 (2006).
20. J. T. Groves, N. Ulman, S. G. Boxer, *Science* **275**, 651 (1997).
21. J. M. Nam, P. M. Nair, R. M. Neve, J. W. Gray, J. T. Groves, *ChemBioChem* **7**, 436 (2006).
22. Materials and methods are available as supporting material on *Science* Online.
23. W. J. Galush, J. A. Nye, J. T. Groves, *Biophys. J.* **95**, 2512 (2008).
24. J.-P. Himanen *et al.*, *Nature* **414**, 933 (2001).
25. B. Day *et al.*, *J. Biol. Chem.* **280**, 26526 (2005).
26. J. P. Himanen *et al.*, *Nat. Neurosci.* **7**, 501 (2004).
27. H. Verschueren, *J. Cell Sci.* **75**, 279 (1985).
28. J. D. Humphries, A. Byron, M. J. Humphries, *J. Cell Sci.* **119**, 3901 (2006).
29. N. Carter, T. Nakamoto, H. Hirai, T. Hunter, *Nat. Cell Biol.* **4**, 565 (2002).
30. M. L. Taddei *et al.*, *Am. J. Pathol.* **174**, 1492 (2009).
31. P. Friedl, K. Wolf, *Nat. Rev. Cancer* **3**, 362 (2003).
32. P. P. Provenzano, D. R. Inman, K. W. Eliceiri, S. M. Trier, P. J. Keely, *Biophys. J.* **95**, 5374 (2008).
33. J. T. Groves, S. G. Boxer, *Acc. Chem. Res.* **35**, 149 (2002).
34. R. M. Neve *et al.*, *Cancer Cell* **10**, 515 (2006).
35. T. Vargo-Gogola, J. M. Rosen, *Nat. Rev. Cancer* **7**, 659 (2007).
36. M. Macrae *et al.*, *Cancer Cell* **8**, 111 (2005).
37. G. Dennis Jr. *et al.*, *Genome Biol.* **4**, P3 (2003).
38. H. Ponta, L. Sherman, P. A. Herrlich, *Nat. Rev. Mol. Cell Biol.* **4**, 33 (2003).
39. We thank N. Bayani for assistance in performing Western blotting, A. Smoligovets and C.-H. Yu for performing transfection and imaging with EGFP-actin–expressing MDA-MB-231 cells, and A. Bershadsky for helpful discussions. This work was supported by the Director, Office of Science, Office of Basic Energy Sciences, Chemical Sciences, Geosciences, and Biosciences Division (K.S., P.M.N.; hybrid synthetic-live cell interfaces) and the Materials Sciences and Engineering Division (R.S.P.; supported membrane substrates) of the U.S. Department of Energy (DOE) under contract no. DE-AC02-05CH11231. Patterned substrate fabrication was performed, in part, at the Molecular Foundry, Lawrence Berkeley National Laboratory (LBNL), and was supported by the Office of Science, Office of Basic Energy Sciences, Scientific User Facilities Division, of the U.S. DOE under contract no. DE-AC02-05CH11231. This work was also supported by the Laboratory Directed Research and Development Program of LBNL under U.S. DOE contract no. DE-AC02-05CH11231. Seed support for biomedical aspects of this work was provided by the U.S. Department of Defense Breast Cancer Research Program Concept Award BC076701 under U.S. Army Medical Research Acquisition Activity no. W81XWH-08-1-0677, with follow-on support provided by Award U54 CA143836 from the National Cancer Institute (NCI) beginning in 2009. The content is solely the responsibility of the authors and does not necessarily represent the official views of the NCI or the NIH. J.W.G. acknowledges support from the Director, Office of Science, Office of Biological and Environmental Research, of the DOE under conract no. DE-AC02-05CH11231; the NIH; NCI grant P50 CA 58207; and the NIH NCI Integrative Cancer Biology Program grant number U54 CA 112970 to J.W.G. (bioinformatics and cell lines). The Regents of the University of California have filed a related patent application through LBNL.

Lgr6 Marks Stem Cells in the Hair Follicle That Generate All Cell Lineages of the Skin

Hugo J. Snippert,[1]* Andrea Haegebarth,[1]* Maria Kasper,[2] Viljar Jaks,[2] Johan H. van Es,[1] Nick Barker,[1] Marc van de Wetering,[1] Maaike van den Born,[1] Harry Begthel,[1] Robert G. Vries,[1] Daniel E. Stange,[1] Rune Toftgård,[2] Hans Clevers[1]†

Mammalian epidermis consists of three self-renewing compartments: the hair follicle, the sebaceous gland, and the interfollicular epidermis. We generated knock-in alleles of murine *Lgr6*, a close relative of the *Lgr5* stem cell gene. *Lgr6* was expressed in the earliest embryonic hair placodes. In adult hair follicles, Lgr6+ cells resided in a previously uncharacterized region directly above the follicle bulge. They expressed none of the known bulge stem cell markers. Prenatal Lgr6+ cells established the hair follicle, sebaceous gland, and interfollicular epidermis. Postnatally, Lgr6+ cells generated sebaceous gland and interfollicular epidermis, whereas contribution to hair lineages gradually diminished with age. Adult Lgr6+ cells executed long-term wound repair, including the formation of new hair follicles. We conclude that Lgr6 marks the most primitive epidermal stem cell.

In the adult skin, interfollicular epidermis (IFE) and sebaceous glands (SGs) are subject to constant self-renewal, whereas hair follicles (HFs) cycle between growth, involution, and resting phases (fig. S1) (*1*). Under normal conditions, these three skin cell populations are each believed to be maintained by their own discrete stem cells (*2*). When tissue homeostasis is disrupted, however, any of the three stem cell populations is capable of producing all three structures (*2*, *3*). The IFE can be maintained without the recruitment of stem cells from the HF bulge (*4–8*), yet the exact identification of IFE stem cells has remained elusive. Within the SG, progenitors reportedly maintain this structure independent of the HF (*5*, *9*). HF stem cells

[1]Hubrecht Institute–KNAW (Royal Netherlands Academy of Arts and Sciences) and University Medical Center Utrecht, Uppsalalaan 8, 3584 CT Utrecht, Netherlands. [2]Karolinska Institutet, Center for Biosciences and Department of Biosciences and Nutrition, Novum, SE-141 57 Huddinge, Sweden.

*These authors contributed equally to this work.
†To whom correspondence should be addressed. E-mail: h.clevers@hubrecht.eu

reside in the bulge, express CD34 and cytokeratin 15 [10–12], and retain DNA or histone labels [13–15]. However, stem cells may reside in other areas of the HF as well [16–19].

We recently identified *Lgr5* [leucine-rich repeat–containing G protein (heterotrimeric guanine nucleotide–binding protein)–coupled receptor 5] as a marker of cycling stem cells in the intestine [20]. Subsequently, we demonstrated that *Lgr5* marks HF stem cells, which over very long periods of time contribute to all hair lineages but not to the SG or IFE [21]. A closely related gene exists in the mammalian genome, *Lgr6* [22]. To evaluate a potential involvement of *Lgr6* in stem cell biology, we obtained *LacZ*- and *EGFP-Ires-CreERT2* (where EGFP is enhanced green fluorescent protein and Ires is internal ribosomal entry site) knock-in alleles [23] (figs. S1 and S2). Both integrations create null alleles. Homozygous mice of both strains were healthy and fertile. In adult *Lgr6LacZ* and *EGFP-Ires-CreERT2* knock-in mice, we noticed prominent expression in rare cells in brain, mammary gland, lung, and skin. In the latter tissue, in situ hybridization confirmed the pattern observed with the knock-in alleles (Fig. 1 and figs. S1 to S3). *Lgr6* was first observed around embryonic day 14.5 (E14.5) (Fig. 1A). Expression was evident throughout the epithelial compartment of placodes, whereas the epidermis was entirely negative (Fig. 1B). Lgr6 is thus one of the earliest placode markers, resembling *Sonic Hedgehog*

[24] and *Sox9* [25]. *Lgr6* expression persisted during hair peg development (Fig. 1C and fig. S2C). The resulting hair breaks through the overlying epidermis postnatally. Lgr6+ cells appeared in the IFE coincident with the emergence of hair (Fig. 1D and fig. S2D), suggesting an origin in the developing follicles. Epidermal *Lgr6* expression peaked around postnatal day 7 to 15 (P7 to P15) and then became gradually more restricted, with expression persisting within adult HFs on the back and tail throughout life (Fig. 1, E and F, and fig. S2, E to I).

Detailed analysis in the first (P20) and second (P56) resting states (telogen) revealed that *Lgr6* marked a unique population, located directly above the CD34 and keratin 15–positive bulge (Figs. 1G and 2A and fig. S1). Lgr6 cells did not retain the DNA label 5-bromo-2′-deoxyuridine (BrdU) (fig. S4). MTS24 and Lrig1 (upper-isthmus markers) [17, 19] and Blimp1 (SG) [9] showed limited overlap with the tight Lgr6 cell cluster (Figs. 1, H and I, and 2A and fig. S1). Analysis of LacZ staining in telogen follicles of *Lgr4* [26], *Lgr5* [20], and *Lgr6* LacZ knock-in mice confirmed that *Lgr6* marked the central isthmus directly above the bulge, whereas *Lgr4* expression was present in both the Lgr5+ and the Lgr6+ domains (Fig. 2B).

In agreement with our findings, gene expression profiles of late embryonic (E17.5) HF stem cells revealed *Lgr5* and *Lgr6* at the top of the enriched-gene list [27]. We directly compared

gene expression profiles of sorted Lgr5^{high} and Lgr6^{high} cells isolated from P20 dorsal skin. As expected, the Lgr5 population was strongly enriched for bulge markers such as CD34 (Fig. 2C). The only gene in the Lgr6 profile implicated in stem cell biology and HF development was *Tnfrsf19/Troy* [28, 29]. Another gene, *Il1r2*, marks cells at a corresponding position below the SGs in human HFs [30]. Thus, Lgr6 marked a unique, tight cell cluster at the central isthmus of the HF (Fig. 2B). Of note, although embryonic expression in nascent whiskers resembled that of other hair follicle types, no Lgr6+ zone was established postnatally at the equivalent location (fig. S9).

To study lineage relationships of Lgr6+ cells, we intercrossed *Lgr6-EGFP-Ires-CreERT2* with the Cre reporter *R26R-LacZ* mice. Without tamoxifen, we essentially noted no leakiness of *Cre* activity. Single tamoxifen injections facilitated genetic tracing of Lgr6+ cells and their offspring. We first genetically marked Lgr6+ cells at E17.5, when Lgr6 expression is restricted to hair pegs (fig. S5A). Subsequent postnatal LacZ stainings were performed at various phases of the hair cycle. In all cases, widespread labeling of all three skin compartments was observed (Fig. 3B and fig. S5).

When lineage tracing was induced at P20, sporadic single LacZ-labeled cells first became visible at P23 (Fig. 3A). The overwhelming majority of labeled cells still appeared at the isthmus,

Fig. 1. Lgr6 is expressed in early hair progenitor cells and becomes restricted to a limited number of cells at the central isthmus. (**A**) Whole-mount picture of a *Lgr6-LacZ* embryo at E14.5. Scale bar indicates 500 μm. (**B** to **F**) Cross sections of dorsal skin from *Lgr6-LacZ* knock-in mice obtained at various developmental stages (E14.5, P1, P7, P20, and P37, respectively) reveal restricted *Lgr6* expression (blue) above the bulge. Scale bars, 50 μm. Confocal microscopy reveals limited overlap with known hair follicle stem cell markers (in red) CD34 (**G**), Mts24 (**H**), and Lrig1 (**I**) in *Lgr6-EGFP-Ires-CreERT2* mice analyzed at telogen stages. Scale bars, 25 μm. Bu, bulge; Sg, sebaceous gland; and UI, upper isthmus.

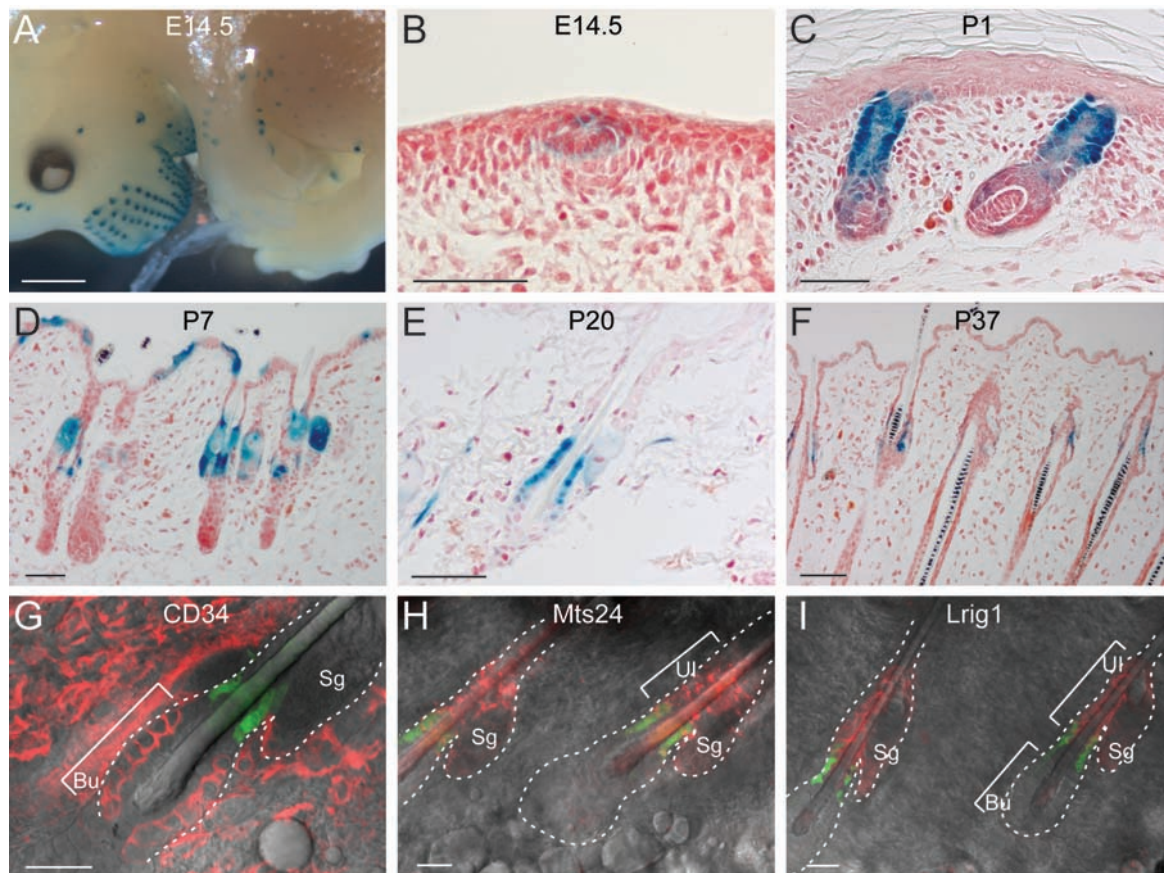**Fig. 2.** Lgr6 marks a different stem cell population than Lgr5/CD34+ HF stem cells. (**A**) Fluorescence-activated cell sorting (FACS) analysis at first telogen reveals that Lgr6+ cells are largely distinct from CD34+ cells and MTS24+ cells. WT, wild type. (**B**) Expression analysis of *Lgr* family members illustrates that Lgr5 HF stem cells are located at the bulge (*21*), whereas *Lgr4* has a wider expression pattern, including the tight cluster of Lgr6+ stem cells at the central isthmus. Scale bar, 50 μm. CI, central isthmus; HG, hair germ; and DP, dermal papilla. (**C**) Gene expression analysis of Lgr5+ HF stem cells and Lgr6+ stem cells further indicates that Lgr6 marks a separate population with no overlap of bulge HF stem cells. Color scale bar represents log$_2$ differences.
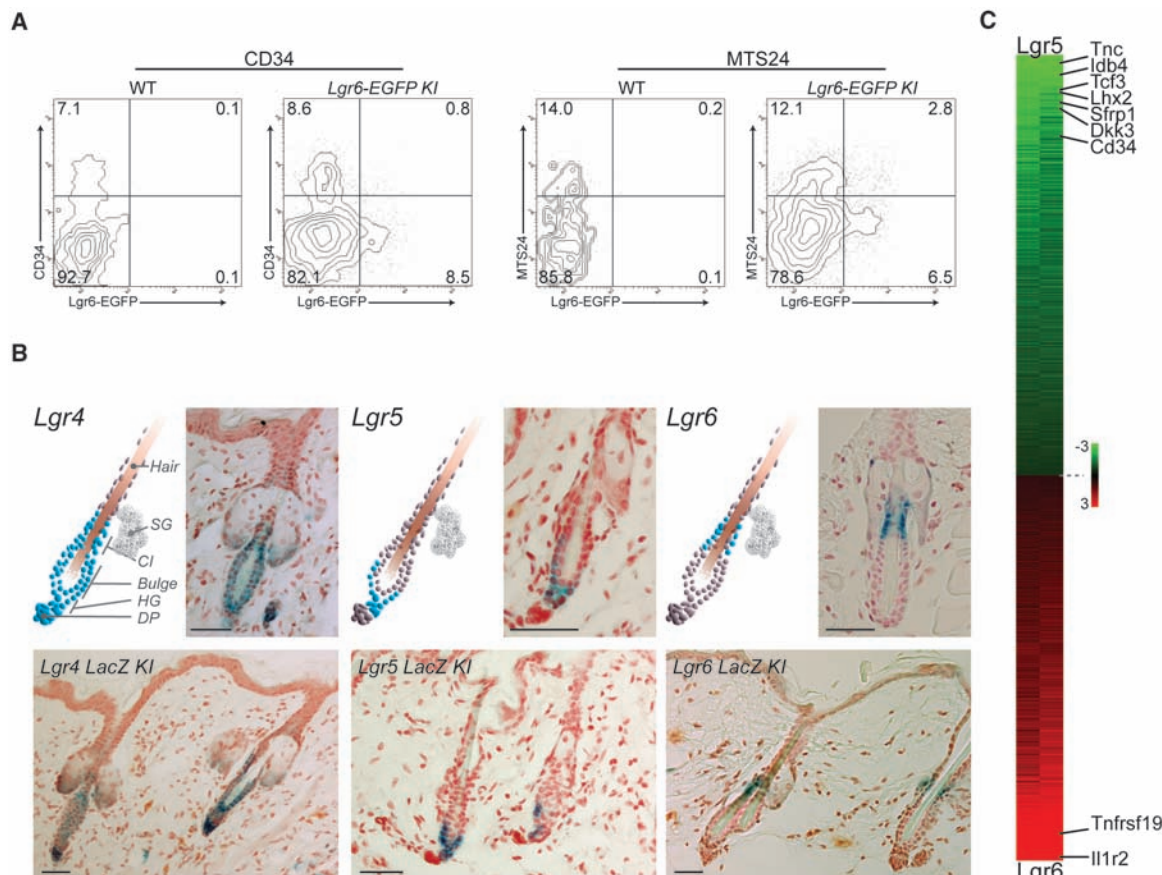

Fig. 3. After hair morphogenesis, Lgr6+ stem cells predominantly generate SGs and epidermis. Scale bars histochemistry (HC), 50 μm. (**A**) LacZ staining (arrow) in dorsal skin, first visible after 3 days of tracing. (**B**) Quantification of lineage tracing from Lgr6 stem cells initiated at E17.5, P20, and P56, respectively. (Left) In postnatal mice, the vast majority of lineage tracings (~90%) originate in the isthmus. (Right) Tracing events remain constant over time and Lgr6 stem cells persistently generate IFE and SG, whereas HF potential diminishes with age of the mice. Error bars indicate standard deviation. (**C** to **E**) LacZ analysis of dorsal skin from *Lgr6-EGFP-Ires-CreERT2/R26R-LacZ* mice after CreERT2 induction at P20. Analysis during anagen at P38 [(C) and (D)] or after >1 year (E) with whole-mount microscopy or HC, respectively. Lgr6+ stem cells persistently trace toward epidermal [(D) and (E), upper left images], SG lineages [(D) and (E), lower left images], and occasional HF [(D) and (E), right images]. (**F**) HC analysis of transplanted Lgr6+/LacZ+ stem cells onto backs of nude mice confirmed multipotency.
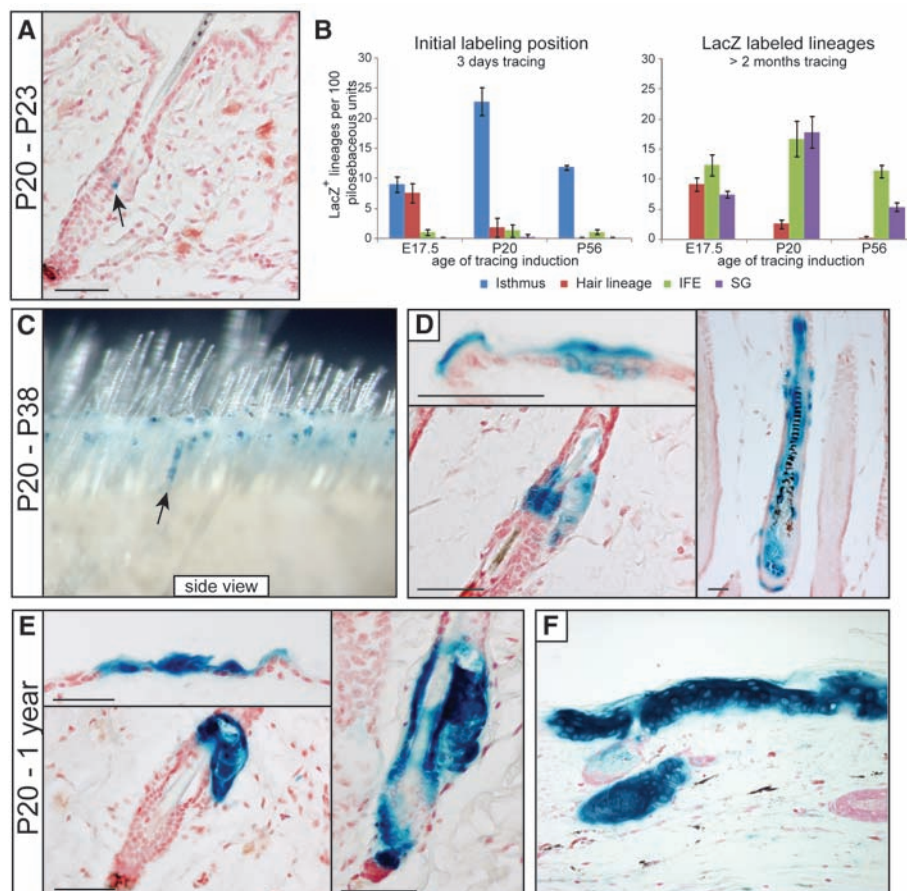
Fig. 4. Lgr6+ stem cells permanently contribute to wound healing, including hair neogenesis. (**A**) Top view of a wound in dorsal skin 2 days postwounding (dpw). White dashed line marks edge of the wound. Incision was made at day P25, 5 days after tracing initiation. Right image is magnification of the area marked by the white box. (**B**) Cross section of the wound reveals marked progeny migrating into the wound. Black arrowhead points to the edge of the wound. Scale bars IHC, 50 μm; Ow, open wound. (**C** and **D**) As in (A) and (B), dorsal wound 7 dpw. (**E** and **F**) As in (A) and (B), 49 dpw Lgr6+ stem cells made persistent contributions. Ki67+ basal layer of scar tissue is Lgr6-derived (black arrows). (**G** and **H**) As in (A) and (B). After >100 dpw, Lgr6 progeny is still present within the wound. Moreover, newly formed hairs within the wound are occasionally LacZ positive.
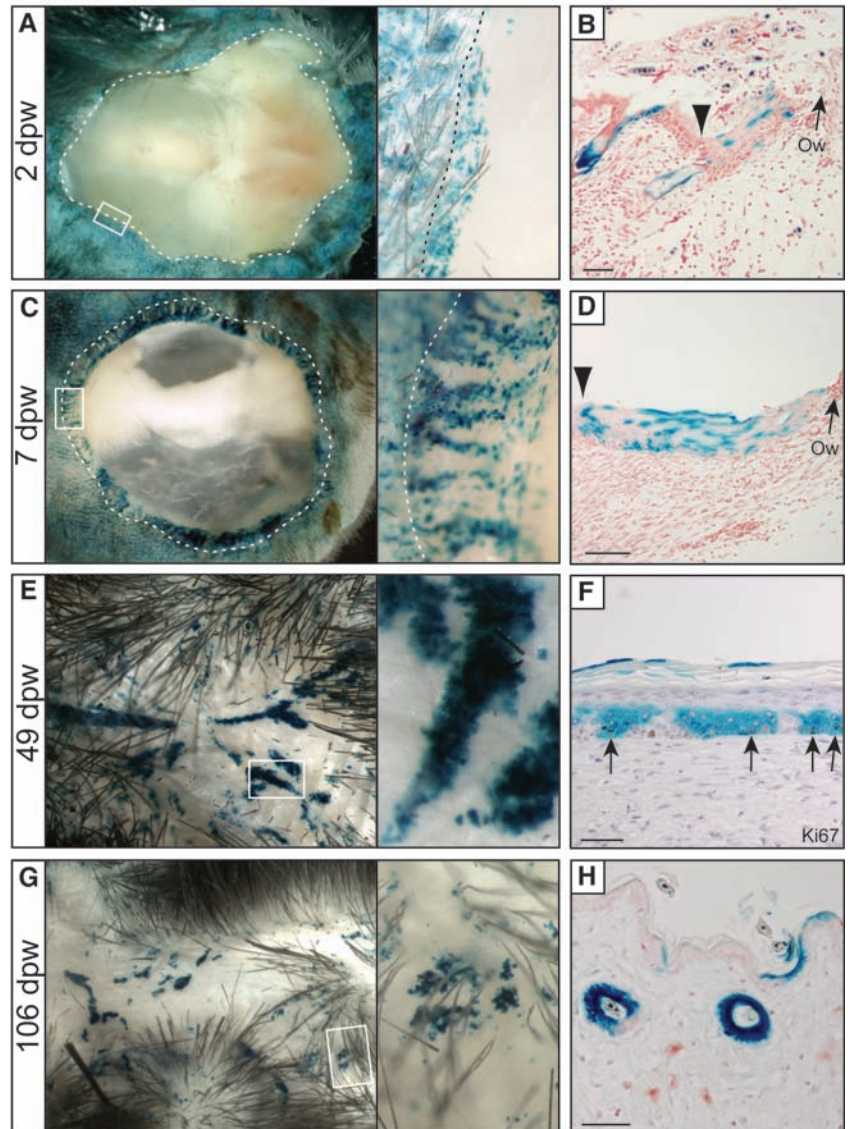
implying limited mobility in the intervening 3-day period (Fig. 3B). When analyzed 18 days after induction, blue clones were observed in SGs, the IFE, and, to a lesser extent, in the hair (Fig. 3, C and D). Even after >1 year, extensive lineage tracing was readily observed (Fig. 3E and fig. S6). Tracing induced at P56, the second telogen phase, yielded identical observations, albeit HF potential was further diminished (Fig. 3B and fig. S7). Quantification of lineage tracing initiated at E17.5, P20, or P56 underscored that, in virtually all cases, labeling was restricted to single cells in the isthmus 3 days after induction (Fig. 3B). Contribution to SG and IFE was relatively constant between E17.5, P20, and P56, whereas the contribution to the hair decreased with age (Fig. 3B).

In order to further document the stemness potential, we transplanted Lgr6+ stem cells, isolated at first telogen, onto the backs of nude mice. As expected, Lgr6+ cells reconstituted fully formed HFs. Multipotency of donor stem cells

was confirmed by activating the *R26R-LacZ* locus in vivo 4 days before isolation. A small subset of Lgr6+ stem cells became LacZ-positive and contributed, once transplanted, to all skin lineages (Fig. 3F and fig. S6F).

The contribution of Lgr6+ cells to wound repair was assessed by inducing lineage tracing at first telogen (P20), followed by excision of 1 cm^2 of full-thickness back skin 5 days later. Lgr6 progeny was traced over >3 months after wounding. As observed previously when bulge stem cells were LacZ-labeled (6), convergent bands of blue cells emanated from the border of the wound and migrated toward its center (Fig. 4, A to D). Such bands originating from HF bulge stem cells disappear by 20 days postwounding (6). The blue clones derived from Lgr6+ cells involved cells in the basal layer of the wound epithelium (Fig. 4, E and F), whereas the clones persisted for >3 months within the newly formed epidermis. As reported by Cotsarelis and colleagues (31), HF growth occurred de novo within the wound epi-

thelium. When scored in a 60- and 100-days postwounding mouse, about 10% of these new HFs were derived from LacZ-marked Lgr6+ stem cells (3 in 34 and 4 in 31, respectively), comparable to the estimated percentage of surface area comprising LacZ-marked keratinocytes in the same wounds (7% and 11%, respectively) (Fig. 4, G and H, and fig. S8).

Our study identifies Lgr6 as a marker for a distinct population of stem cells giving rise to all lineages of the skin. Unlike the *Lgr5* gene, we found no evidence that *Lgr6* is controlled by Wnt signaling. This is in agreement with the notion that the active hair lineage in the lower bulge requires Wnt signaling, whereas the sebaceous and epidermal lineages are Wnt-independent (2). A picture thus emerges in which a Wnt-independent Lgr6 stem cell pool can renew sebaceous cells and seed the epidermis throughout life, whereas a Wnt-dependent Lgr5 stem cell pool derives from the Lgr6 pool early in life but then becomes relatively independent.

References and Notes

1. L. Alonso, E. Fuchs, *J. Cell Sci.* **119**, 391 (2006).
2. E. Fuchs, V. Horsley, *Genes Dev.* **22**, 976 (2008).
3. V. Levy, C. Lindon, Y. Zheng, B. D. Harfe, B. A. Morgan, *FASEB J.* **21**, 1358 (2007).
4. S. Claudinot, M. Nicolas, H. Oshima, A. Rochat, Y. Barrandon, *Proc. Natl. Acad. Sci. U.S.A.* **102**, 14677 (2005).
5. S. Ghazizadeh, L. B. Taichman, *EMBO J.* **20**, 1215 (2001).
6. M. Ito *et al.*, *Nat. Med.* **11**, 1351 (2005).
7. V. Levy, C. Lindon, B. D. Harfe, B. A. Morgan, *Dev. Cell* **9**, 855 (2005).
8. E. Clayton *et al.*, *Nature* **446**, 185 (2007).
9. V. Horsley *et al.*, *Cell* **126**, 597 (2006).
10. C. S. Trempus *et al.*, *J. Invest. Dermatol.* **120**, 501 (2003).
11. C. Blanpain, W. E. Lowry, A. Geoghegan, L. Polak, E. Fuchs, *Cell* **118**, 635 (2004).
12. R. J. Morris *et al.*, *Nat. Biotechnol.* **22**, 411 (2004).
13. G. Cotsarelis, T. T. Sun, R. M. Lavker, *Cell* **61**, 1329 (1990).
14. K. M. Braun *et al.*, *Development* **130**, 5241 (2003).
15. T. Tumbar *et al.*, *Science* **303**, 359 (2004); published online 11 December 2003 (10.1126/science.1092436).
16. M. Ito, K. Kizawa, K. Hamada, G. Cotsarelis, *Differentiation* **72**, 548 (2004).
17. J. G. Nijhof *et al.*, *Development* **133**, 3027 (2006).
18. U. B. Jensen *et al.*, *J. Cell Sci.* **121**, 609 (2008).
19. K. B. Jensen *et al.*, *Cell Stem Cell* **4**, 427 (2009).
20. N. Barker *et al.*, *Nature* **449**, 1003 (2007).
21. V. Jaks *et al.*, *Nat. Genet.* **40**, 1291 (2008).
22. T. Van Loy *et al.*, *Gen. Comp. Endocrinol.* **155**, 14 (2008).
23. Materials and methods are available as supporting material on *Science* Online.
24. S. Iseki *et al.*, *Biochem. Biophys. Res. Commun.* **218**, 688 (1996).
25. V. P. Vidal *et al.*, *Curr. Biol.* **15**, 1340 (2005).
26. G. Van Schoore, F. Mendive, R. Pochet, G. Vassart, *Histochem. Cell Biol.* **124**, 35 (2005).
27. H. Rhee, L. Polak, E. Fuchs, *Science* **312**, 1946 (2006).
28. L. G. van der Flier *et al.*, *Cell* **136**, 903 (2009).
29. J. Pispa, M. Pummila, P. A. Barker, I. Thesleff, M. L. Mikkola, *Hum. Mol. Genet.* **17**, 3380 (2008).
30. M. Kasper *et al.*, *Mol. Cell. Biol.* **26**, 6283 (2006).
31. M. Ito *et al.*, *Nature* **447**, 316 (2007).
32. We acknowledge M. Cozijnsen, J. Korving, Å. Bergström, Å. Dackland, and Hubrecht Imaging Centre for technical help and support. This work was supported by the Koningin Wilhelmina Fonds and a European Research Council grant to H.C., a European Molecular Biology Organization Long-Term Fellowship to A.H., and by grants from the Swedish Cancer Society and the Swedish Research Council to R.T. A patent is pending on work with Lgr5 and Lgr6 (A.H., N.B., and H.C.). GEO microarray accession number is GSE20269.

Structural Sources of Robustness in Biochemical Reaction Networks

Guy Shinar[1] and Martin Feinberg[2]*

In vivo variations in the concentrations of biomolecular species are inevitable. These variations in turn propagate along networks of chemical reactions and modify the concentrations of still other species, which influence biological activity. Because excessive variations in the amounts of certain active species might hamper cell function, regulation systems have evolved that act to maintain concentrations within tight bounds. We identify simple yet subtle structural attributes that impart concentration robustness to any mass-action network possessing them. We thereby describe a large class of robustness-inducing networks that already embraces two quite different biochemical modules for which concentration robustness has been observed experimentally: the *Escherichia coli* osmoregulation system EnvZ-OmpR and the glyoxylate bypass control system isocitrate dehydrogenase kinase-phosphatase–isocitrate dehydrogenase. The structural attributes identified here might confer robustness far more broadly.

Biological systems require robustness, that is, the capacity for sustained and precise function even in the presence of structural or environmental disruption (*1–11*). Examples of robustness exist over multiple scales of biological organization, from the biochemical circuit level [robust exact adaptation in bacterial chemotaxis (*2–4*)] to the cellular level [robustness of metabolic functions to changes caused by mutations (*12*)].

A biological system shows absolute concentration robustness (ACR) for an active molecular species if the concentration of that species is identical in every positive steady state the system might admit. The function of an ACR-possessing system is thereby protected even against large changes in the overall supply of the system's components.

[1]Department of Molecular Cell Biology, Weizmann Institute of Science, Rehovot 76100, Israel. [2]William G. Lowrie Department of Chemical and Biomolecular Engineering and Department of Mathematics, Ohio State University, 125 Koffolt Laboratories, 140 West 19th Avenue, Columbus, OH 43210, USA.

*To whom correspondence should be addressed. E-mail: feinberg@chbmeng.ohio-state.edu

We identify simple yet subtle structural attributes that will impart ACR to any mass-action network that includes them. We provide a mathematical theorem that precisely delineates a very large class of ACR-possessing systems, a class that embraces networks that differ in size, detail, and complexity. This class contains different ACR-possessing models (*9, 11*) of known examples for which approximate concentration robustness has been verified experimentally. We thus uncover an underlying mathematical unity found at the heart of robustness-producing mechanisms that are biochemically quite different.

To elucidate the concept of ACR, we first consider the toy two-species mass-action system

$$A + B \xrightarrow{\alpha} 2B$$
$$B \xrightarrow{\beta} A \tag{1}$$
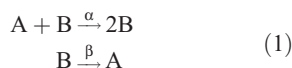
where A is the active form of a protein, B is the inactive form, and α and β are rate constants. Suppose the protein is synthesized and degraded over long time scales, so that the total protein concentration can be regarded as constant over

the system's equilibrium time scale. Under this assumption, the differential equations governing the time evolution of the molar concentrations of A and B, denoted c_A and c_B, are

$$\dot{c}_A = -\alpha c_A c_B + \beta c_B$$
$$\dot{c}_B = \alpha c_A c_B - \beta c_B \tag{2}$$

The positive steady states of Eq. 2 are given by

$$c_A = \frac{\beta}{\alpha}$$
$$c_B = \Theta - \frac{\beta}{\alpha} \tag{3}$$

where Θ is the conserved total protein concentration: $\Theta = c_A + c_B = c_A(0) + c_B(0)$. Eq. 3 shows that system (1) has ACR: There is a positive steady state for each value of Θ exceeding β/α, and in each of these steady states c_A has precisely the same value.

In contrast, consider the simple module

$$A \underset{\beta}{\overset{\alpha}{\rightleftarrows}} B \tag{4}$$

Here, the positive steady states are given by

$$c_A = \frac{\beta\Theta}{\alpha + \beta}$$
$$c_B = \frac{\alpha\Theta}{\alpha + \beta} \tag{5}$$

The steady state values of both c_A and c_B are proportional to the conserved total concentration $\Theta = c_A + c_B$. Thus, as Θ varies, both c_A and c_B vary in step. The system does not have ACR.

To state our main result, we require some terminology from chemical reaction network theory (*13–16*). The display in Fig. 1A is an example of a standard reaction diagram, that is, a directed graph whose nodes (*17*) are the distinct linear combinations of chemical species that sit at the heads and tails of the reaction arrows. In Fig. 1A, the chemical species are A, B, C, D, E, and F,

Science

Lgr6 Marks Stem Cells in the Hair Follicle That Generate All Cell Lineages of the Skin

Hugo J. Snippert, Andrea Haegebarth, Maria Kasper, Viljar Jaks, Johan H. van Es, Nick Barker, Marc van de Wetering, Maaike van den Born, Harry Begthel, Robert G. Vries, Daniel E. Stange, Rune Toftgård and Hans Clevers

Hair Today, Skin Tomorrow

The epidermis of mammals contains hair follicles, sebaceous glands, and interfollicular epidermis, but it has not been clear how the development and repair of these structures is regulated. **Snippert *et al.*** (p. 1385) show that a stem-cell cluster in the hair follicle, characterized by the expression of Lgr6, a close homolog of the Lgr5 marker for stem cells in the small intestine and colon, resides directly above the hair bulge and gives rise to all cell lineages of the skin. Skin wounds in adult mice are repaired by Lgr6 stem cells in the hair follicles that flank the damage. After hair morphogenesis, Lgr6 stem cells give rise to epidermal and sebaceous gland lineages to generate fully differentiated new skin.

ARTICLE TOOLS	http://science.sciencemag.org/content/327/5971/1385
SUPPLEMENTARY MATERIALS	http://science.sciencemag.org/content/suppl/2010/03/09/327.5971.1385.DC1
REFERENCES	This article cites 30 articles, 11 of which you can access for free http://science.sciencemag.org/content/327/5971/1385#BIBL
PERMISSIONS	http://www.sciencemag.org/help/reprints-and-permissions

Use of this article is subject to the Terms of Service